Three Octave Six-Port Network for a Broadband Software Radio Receiver

Cristina de la Morena-Álvarez-Palencia[#1], Mateo Burgos-García[#2], David Rodríguez-Aparicio[#3]

[#]*Department of Signals, Systems and Radiocommunications, Universidad Politécnica de Madrid*

Ciudad Universitaria s/n, 28040, Madrid

[1]cmorena@gmr.ssr.upm.es

[2]mateo@gmr.ssr.upm.es

[3]david.rodriguez.aparicio@alumnos.upm.com

***Abstract*—The six-port network has been identified in recent years as the best candidate to implement a Software Defined Radio (SDR). However, it is difficult in practice to implement a device without impairments if a broadband design is addressed. In this paper we present a three octave six-port network, covering the frequency range from 698 MHz to 5850 MHz. The six-port network is part of a SDR receiver prototype for a novel broadband mobile communications system. It has been measured with good performance.**

I. INTRODUCTION

Initially, the six-port network was introduced as an alternative network analyzer in the seventies [1]. It was in 1994 when the six-port network was first used as a communication receiver [2]. From that moment on, this promising structure has been using for many applications: radar systems [3], direction of arrival estimation [4], UWB (Ultra-Wide-Band) [5], MIMO (Multiple Input Multiple Output) systems [6], etc. But it is especially interesting its application to an emerging radio concept: the Software Defined Radio (SDR) [7].

The six-port receiver is a zero-IF architecture, which is one of the most interesting techniques for SDR due to its advantages: no image frequency, no bulky intermediate frequency (IF) components, low cost, high level of integration, flexibility, and reconfigurability. The six-port architecture does not use an I-Q mixer for the frequency conversion, so it has the zero-IF advantages without I-Q mixer problems. The main advantage of the six-port network is its extremely large bandwidth, providing multi-band and multi-standard capabilities. In addition, it can be implemented in MMIC or LTTC technology, with compact size and low cost productions for configurable radio terminals.

Due to all these advantages, we have chosen the six-port architecture to develop a SDR prototype for broadband mobile applications. We will present in this paper the design and implementation of the six-port network.

II. PRINCIPLE OF OPERATION OF SIX-PORT ARCHITECTURE

The principle of operation of the six-port network as a zero-IF receiver is based on the measurement of four independent power observations, when radiofrequency (RF) and local oscillator (LO) signals are introduced into the other two ports [8]. A power detector and a low-pass filter are located at each out port, as shown in Fig.1.

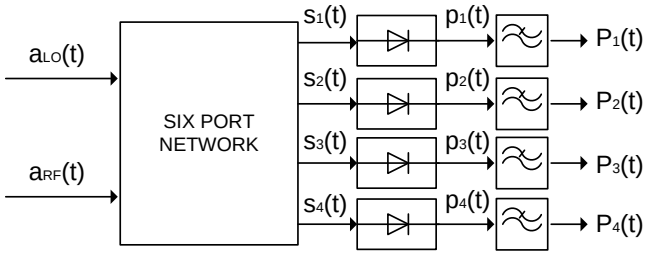

Fig. 1 Zero-IF receiver based on six-port network

In order to understand the six-port architecture behaviour, let us consider the next two input signals:

$$a_{LO}(t) = A_{LO}\cos(2\pi f_{LO}t + \phi_{LO}) \quad (1)$$

$$a_{RF}(t) = A_{RF}(t)\cos(2\pi f_{RF}t + \phi_{RF}(t)) \quad (2)$$

Being $a_{LO}(t)$ the local oscillator signal, and $a_{RF}(t)$ the I-Q modulated RF signal. Six-port network is a passive and linear network, so output signals s_i are linear combinations of the input signals:

$$s_i(t) = A_i A_{LO}\cos(2\pi f_{LO}t + \phi_{LO} + \phi_{A_i}) + B_i A_{RF}(t)\cos(2\pi f_{RF}t + \phi_{RF}(t) + \phi_{B_i}) \quad (3)$$

With i={3,…,6}. A_i, B_i, Φ_{Ai}, and Φ_{Bi} are constant values depending on the six-port scattering parameters and the frequency of operation. The power detector has a response described by the next expression:

$$p_i(t) = K_0 + K_1 \cdot s_i(t) + \frac{K_2}{2}\cdot s_i(t)^2 + \frac{K_3}{3}\cdot s_i^3(t) + \ldots \quad (4)$$

Substituting (3) into (4), we obtain the instantaneous power at the detectors outputs:

$$p_i(t) = K_0 + K_1\left[A_i A_{LO}\cos(2\pi f_{LO}t + \phi_{LO} + \phi_{A_i}) + B_i A_{RF}(t)\cos(2\pi f_{RF}t + \phi_{RF}(t) + \phi_{B_i})\right] +$$
$$\frac{K_2}{4}\left[A_i^2 A_{LO}^2 + B_i^2 A_{RF}^2(t)\right] + \frac{K_2}{2}\left[A_i A_{LO} B_i A_{RF}(t)\cos(2\pi(f_{LO} - f_{RF})t + \gamma(t))\right] +$$
$$\frac{K_2}{2}\left[A_i A_{LO} B_i A_{RF}(t)\cos(2\pi(f_{LO} + f_{RF})t + \gamma(t))\right] +$$
$$\frac{K_2}{4}\left[A_i^2 A_{LO}^2\cos(2\pi 2f_{LO}t + \phi_{LO} + \phi_{A_i}) + B_i^2 A_{RF}^2(t)\cos(2\pi 2f_{RF}t + \phi_{RF}(t) + \phi_{B_i})\right] + \ldots \quad (5)$$

With:

$$\gamma(t) = \phi_{LO} + \phi_{A_i} - \phi_{RF}(t) - \phi_{B_i} \quad (6)$$

Final published version of the paper in Proc. of 40th European Microwave Conference (EuMC 2010), Paris, France, pp. 1110-1113, 28-30/09/2010. ISBN 978-2-87487-016-3, Print ISBN 978-1-4244-7232-1. doi: 10.23919/EUMC.2010.5616435. Accesible in: https://ieeexplore.ieee.org/document/5616435.

Six-port receiver is a zero-IF architecture, that is, LO frequency is equal to RF. Therefore, after low-pass filtering, the signal becomes:

$$P_i(t) = K_0 + \frac{K_2}{4} A_i^2 A_{LO}^2 + \frac{K_2}{4} B_i^2 A_{RF}^2(t) + \frac{K_2}{2}\left[A_i A_{LO} B_i A_{RF}(t)\cos(\gamma(t))\right] \quad (7)$$

Each output signal contains a DC term, whose predominant component is the self-mixing of the local oscillator, the self-mixing of the modulated signal, and the desired signal. It is convenient to eliminate the DC term, as it can saturate next stages, as the A/D converters. In addition, the six-port architecture is a direct conversion architecture, so DC-offset distorts the received signal. A digital DC-offset cancellation is also required.

Original I-Q components are regenerated from the four power measurements and some calibration constants depending on the system response.

$$I(t) = h_3 \cdot \tilde{P}_3(t) + h_4 \cdot \tilde{P}_4(t) + h_5 \cdot \tilde{P}_5(t) + h_6 \cdot \tilde{P}_6(t) \quad (8)$$

$$Q(t) = q_3 \cdot \tilde{P}_3(t) + q_4 \cdot \tilde{P}_4(t) + q_5 \cdot \tilde{P}_5(t) + q_6 \cdot \tilde{P}_6(t) \quad (9)$$

The objective of the calibration process is to determine these calibration constants. Calibration process is a key factor in the six-port architecture.

III. Six-Port Network Design

The objective is to implement a software configurable receiver prototype, with multi-band and multi-standard capabilities for broadband mobile applications. Nowadays, the aim of a SDR for mobile applications can be reduced to receive every standard up to 6 GHz, approximately, where all cellular and WLAN communications are located. A six-port network covering the frequency range from 698 MHz to 5850 MHz (three octave bandwidth) will be designed. Although it is not presented in this paper, the entire receiver has been developed, including a low noise amplifier, RF filters and wideband power detectors. Fig. 2 shows the structure of the six-port network. It consists on a power divider and three 3dB quadrature couplers.

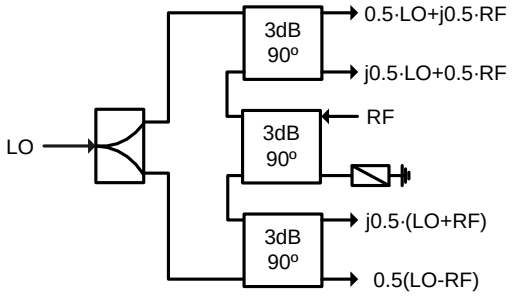

Fig. 2 Six-port network topology

The system bandwidth is conditioned by the hybrid couplers, as they must ensure a frequency independent phase shift. The greatest difficulty is to design a 3 dB coupler over three octave bandwidth. Branch-line and rate-race couplers are suitable for obtaining tight coupling values, such as 3 dB. However, these couplers are inherently narrowband circuits (<20% bandwidth). The use of 3 dB Lange couplers enhances the bandwidth, but only up to one octave. A tight coupler can also be obtained by connecting two couplers in tandem. In a tandem connection, the direct and coupled ports of the first coupler are connected to the isolated and input ports of the second coupler, respectively. The tandem connection of two 8.34 dB couplers gives rise to a 3 dB coupler [9]. A three octave 3 dB coupler can be obtained from two 8.34 dB multisection couplers. From the design tables [10], we obtain that it is possible to cover the specified bandwidth with five $\lambda/4$ sections and a ripple of 0.7 dB. With seven $\lambda/4$ sections it is possible to achieve a 0.3 dB ripple. In a good six-port network design it is convenient to minimise amplitude imbalance, so seven $\lambda/4$ sections are more appropriate. In this case, the highest coupling level required by the design is 3.8 dB, which corresponds to the central section coupling. Edge-coupled structures do not provide coupling levels higher than 8 dB. Broadside-coupled lines are more suitable, as they achieve coupling levels up to 2 or 3 dB. In conclusion, we will implement a seven section 3 dB tandem coupler with broadside-coupled striplines.

The decision of the substrate parameters is conditioned by the central section coupling level. Coupling can be maximised by reducing the separation of the inner conductors, and increasing the distance to the ground planes. A low dielectric constant substrate also maximises the highest coupling, as the ground plane separation will be large relative to the overlay separation. However, this increases the circuit dimension. We have chosen a ε_r=2.17 Cu-Clad substrate, with 380 µm inner conductor separation, and 1143 µm ground separation. The central section coupling is achieved with 50 Ω overlap broadside-coupled striplines. The layout of the designed coupler is shown in Fig. 3. The circuit dimensions are 130x17 mm.

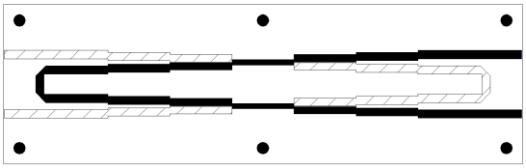

Fig. 3 Layout of the 3 dB tandem coupler in stripline technology.

Fig. 4 illustrates a photograph of one of the three constructed couplers. The structure is formed by a 1143-380-1143 sandwich of 2.17 Cu-Clad substrate, where metallization lines are printed on the top and bottom side of the central layer in order to reduce alignment errors.

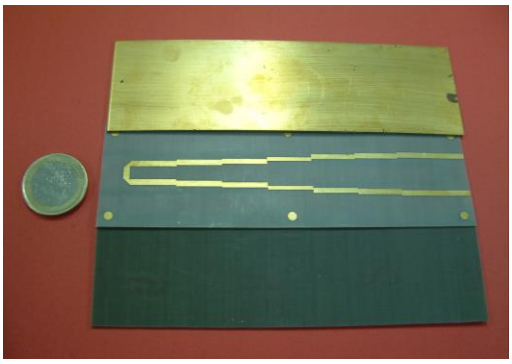

Fig. 4 Photograph of 3 dB tandem coupler in stripline technology.

Final published version of the paper in Proc. of 40th European Microwave Conference (EuMC 2010), Paris, France, pp. 1110-1113, 28-30/09/2010. ISBN 978-2-87487-016-3, Print ISBN 978-1-4244-7232-1. doi: 10.23919/EUMC.2010.5616435.
Accesible in: https://ieeexplore.ieee.org/document/5616435.

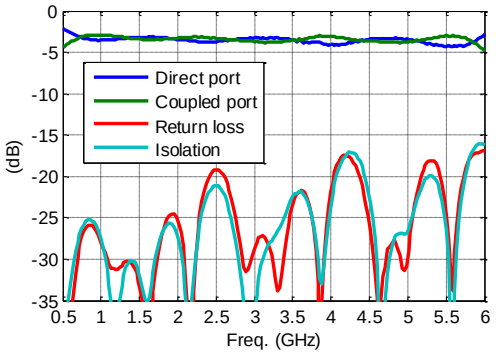

Fig. 5 Measured frequency response of 3dB tandem coupler.

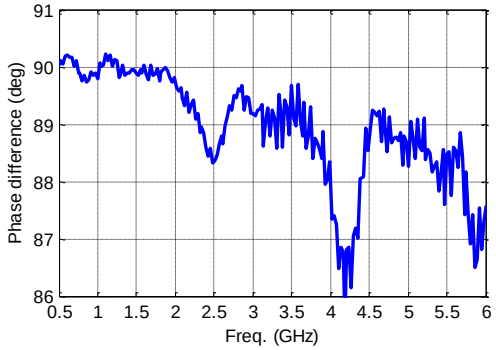

Fig. 6 Measured phase difference between direct and coupled ports of 3 dB tandem coupler.

The couplers have been characterized with good performance. Fig. 5 and Fig.6 present the coupler amplitude and phase frequency response, respectively. Input return loss and isolation are better than 15 dB over the entire bandwidth. The maximum phase imbalance is 4º, and the maximum amplitude imbalance is 1.2 dB.

The entire six-port network can be seen in Fig. 7. The three 3 dB couplers have been assembled over a metallic structure. They are interconnected by external coaxial cables, which must have the same length in order to preserve the six-port phase behaviour. The power divider is the *Tiger TGP-A0214* divider. It is connected to the couplers by two coaxial cables, which must be identical.

Fig. 7 Six-port network physical realization.

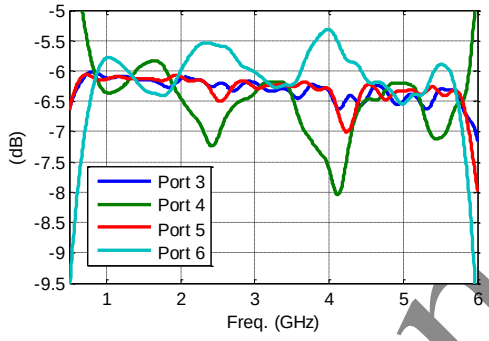

(a)

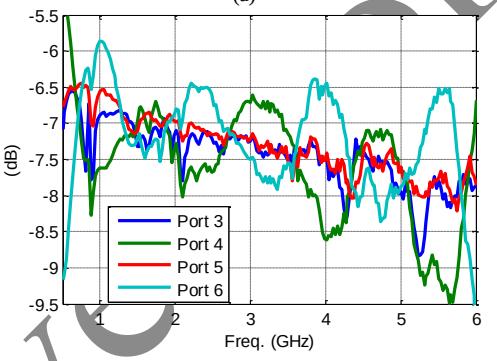

(b)

Fig. 8 Attenuation from RF port to output ports (a) Simulated (b) Measured.

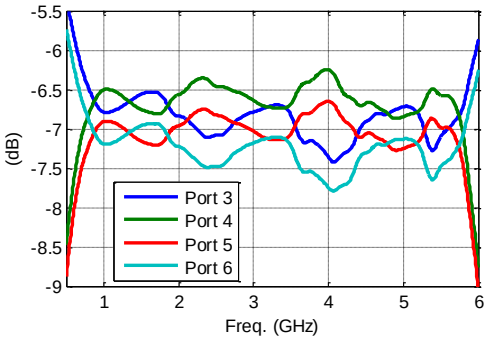

(a)

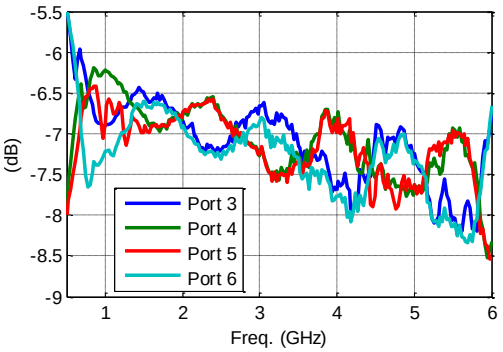

(b)

Fig. 9 Attenuation from LO port to output ports (a) Simulated (b) Measured.

IV. Six-Port Simulation and Measurements Results

This section describes the characterization of the developed six-port network. Both simulated and measured results are presented. Simulations have been realized using ADS Momentum.

Final published version of the paper in Proc. of 40th European Microwave Conference (EuMC 2010), Paris, France, pp. 1110-1113, 28-30/09/2010. ISBN 978-2-87487-016-3, Print ISBN 978-1-4244-7232-1. doi: 10.23919/EUMC.2010.5616435. Accesible in: https://ieeexplore.ieee.org/document/5616435.

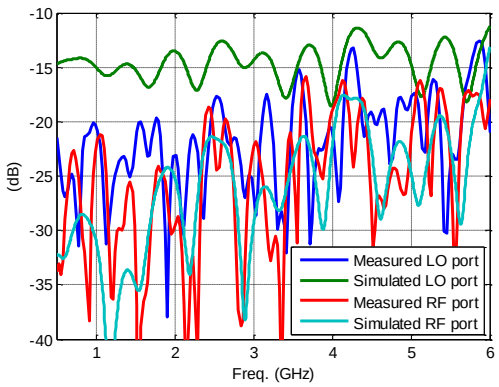

Fig. 10 Simulated and measured input return loss at LO and RF ports.

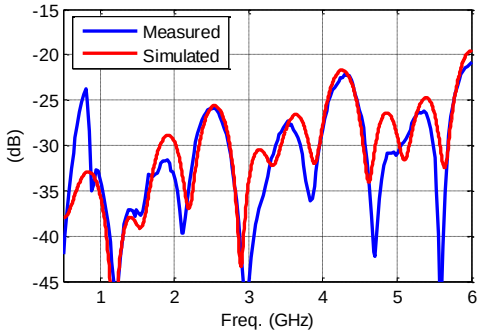

Fig. 11 Simulated and measured isolation between LO and RF ports.

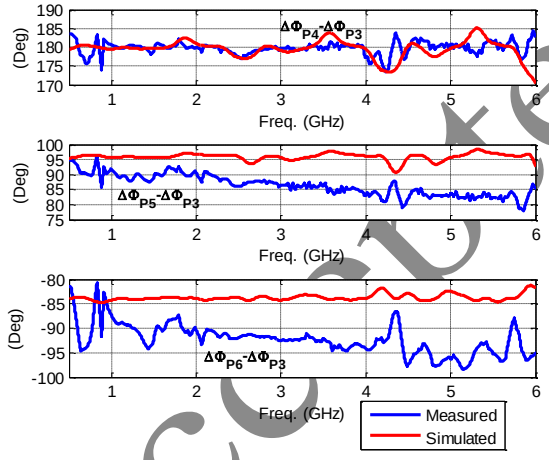

Fig. 12 Simulated and measured phase response.

The attenuations from LO and RF ports to output ports are shown in Fig. 8 and Fig.9. Ideally, these attenuations are -6 dB. The measured attenuation curves present a loss factor that increases with the increase of frequency, in part due to the interconnection coaxial cables. Best results would be obtained with LTCC technology, as the components can be internally interconnected, in addition to more compact size. At present we are working on a new version of the six-port network based on LTCC technology.

Fig. 10 and Fig. 11 illustrate input return loss and isolation, respectively. Input return losses at LO and RF port are below -20 dB up to 2.4 GHz. From 2.4 GHz to 6 GHz, input return loss at RF port is below -16 dB, and below -13 dB for the LO port. Simulated and measured isolation curves bear strong resemblance. Measured isolation is better than 20 dB over the whole bandwidth.

To analyse the six-port phase behaviour, we will define the parameter $\Delta\Phi_{Pi}$ as the phase difference between S_{i2} and S_{i1}, with i=3,…,6. According to the chosen six-port topology (see Fig. 2), $\Delta\Phi_{Pi}$ parameters must be 180º, 90º and -90º phase shifted each other. The phase shifts referred to $\Delta\Phi_{P3}$ are presented in Fig. 12. Measured results show a maximum error of 10º compared to the theoretical behaviour.

V. Conclusions

The six-port architecture reemerges from the search of low-cost, multi-band and multi-standard transceivers. Its inherent advantages, especially its broadband behaviour, make this a structure a good candidate to implement a SDR. In this paper, we have described the background and fundamentals of the six-port technique. We have presented a three octave bandwidth six-port network, which is part of a SDR receiver prototype for broadband mobile applications. The system has been measured with good performance. Currently an LTCC version of the network is under development in order to miniaturize the design.

Acknowledgment

This work has been funded by the Spanish National Board of Scientific and Technological Research (CICYT), under project contract TEC2008-02148, and by CDTI and INDRA SISTEMAS, under TelMAX project inside CENIT program.

References

[1] G.F. Engen, "The six-port reflectometer an alternative network analyzer," *IEEE Trans. Microwave Theory Tech.*, vol. MTT-25, pp. 1075–1079, Dec. 1977.

[2] J. Li, R.G. Bosisio, and K. Wu, "A six-port direct digital millimeter-wave receiver," *IEEE MTT-S Int. Microwave Symp. Dig.*, San Diego, CA, vol. 3, pp. 1659–1662, 23-27 May 1994.

[3] H. Zhang, L. Li, and K. Wu, "Software-Defined Six-Port Radar Technique for Precision Range Measurements," *IEEE Sensors Journal*, vol.8, no.10, pp.1745-1751, Oct. 2008.

[4] V.Y Vu, A.J. Braga, X. Begaud, and B. Huyart, "Measurement of direction-of-arrival of coherent signals using five-port reflectometers and quasi-Yagi antennas," *IEEE Microwave and Wireless Components Letters*, vol.15, no.9, pp. 558-560, Sept. 2005.

[5] R.G. Bosisio, Y.Y. Zhao, X.Y. Xu, S. Abielmona, E. Moldovan, Y.S. Xu, M. Bozzi, S.O. Tatu, C. Nerguizian, J.F. Frigon, C. Caloz, and K. Wu, "New-Wave Radio," *IEEE Microwave Magazine*, vol.9, no.1, pp.89-100, Feb. 2008.

[6] K. Mabrouk, B. Huyart, X. Begaud, and A.B. Mohammed, "Baseband to baseband calibration of a MIMO wireless system," *2007 European Conference on Wireless Technologies*, vol., no., pp.142-145, 8-10 Oct. 2007.

[7] J.-F. Luy, T. Mueller, T. Mack, and A. Terzis, "Configurable RF receiver architectures," *IEEE Microwave Magazine*, vol.5, no.1, pp. 75-82, Mar 2004.

[8] T. Hentschel, "The six-port as a communications receiver," *IEEE Trans. Microwave Theory Tech.*, vol.53, no.3, pp. 1039-1047, March 2005.

[9] R. K. Mongia, I. J. Bahl, P. Barthia, and J. Hong, *RF and Microwave Coupled-Line Circuits*, 2nd ed., Artech House Inc., 2007.

[10] E. G. Cristal and L. Young, "Theory and tables of Optimum Symmetrical TEM-Mode Coupled-Transmission-Line Directional Couplers," *IEEE Trans. Microwave Theory Tech.*, vol. MTT-13, pp. 544-558, Sept. 1965.

Final published version of the paper in Proc. of 40th European Microwave Conference (EuMC 2010), Paris, France, pp. 1110-1113, 28-30/09/2010. ISBN 978-2-87487-016-3, Print ISBN 978-1-4244-7232-1. doi: 10.23919/EUMC.2010.5616435. Accesible in: https://ieeexplore.ieee.org/document/5616435.